Vision Research 179 (2021) 75–84

Contents lists available at ScienceDirect

Vision Research

journal homepage: www.elsevier.com/locate/visres

Adaptation to geometrically skewed moving images: An asymmetrical effect on the double-drift illusion

Miguel Garcia Garcia [a,b,c,*], Katharina Rifai [a,b], Siegfried Wahl [a,b], Tamara Watson [c]

[a] Carl Zeiss Vision International GmbH, Turnstrasse 27, 73430 Aalen, Germany
[b] Institute for Ophthalmic Research, Eberhard Karls University Tuebingen, Tuebingen 72076, Germany
[c] School of Psychology, Western Sydney University, New South Wales 2214, Australia

ARTICLE INFO

Keywords:
Skew distortions
Curveball
Illusion
Adaptation
Progressive lenses
Optic flow

ABSTRACT

Progressive addition lenses introduce distortions in the peripheral visual field that alter both form and motion perception. Here we seek to understand how our peripheral visual field adapts to complex distortions. The adaptation was induced across the visual field by geometrically skewed image sequences, and aftereffects were measured via changes in perception of the double-drift illusion. The double-drift or curveball stimulus contains both local and object motion. Therefore, the aftereffects induced by geometrical distortions might be indicative of how this adaptation interacts with the local and object motion signals.

In the absence of the local motion components, the adaptation to skewness modified the perceived trajectory of object motion in the opposite direction of the adaptation stimulus skew. This effect demonstrates that the environment can also tune perceived object trajectories. Testing with the full double-drift stimulus, adaptation to a skew in the opposite direction to the local motion component induced a change in perception, reducing the illusion magnitude (when the stimulus was presented on the right side of the screen. A non-statistically significant shift, when stimuli were on the left side). However, adaptation to the other orientation resulted in no change in the strength of the double-drift illusion (for both stimuli locations). Thus, it seems that the adaptor's orientation and the motion statistics of the stimulus jointly define the perception of the measured aftereffect.

In conclusion, not only size, contrast or drifting speed affects the double-drift illusion, but also adaptation to image distortions.

1. Introduction

The visual cortex is able to self-calibrate (Barlow and Földiák, 1989), adapting to ensure it can respond to the continuously changing properties of the environment. Changes in the optical properties of the eye and subsequent optical correction with lenses both create a need for adaptation within the visual brain. For example, the visual system's adaptive techniques allow it to be more efficient under certain circumstances such as blur (Webster, Georgeson, & Webster, 2002), astigmatism (Ohlendorf, Tabernero, & Schaeffel, 2011), magnifications (Adams, Banks, & van Ee, 2001), or skew distortions (Habtegiorgis, Rifai, Lappe, & Wahl, 2017) that can be altered with the use of spectacles.

When considering adaptation, progressive addition lenses (PALs) are a particularly interesting form of optical correction. PALs provide presbyopes with clear vision at different distances wearing only one pair of spectacles (Poullain & Cornet, 1911). This optical solution has become increasingly popular in the last decades (Meister & Fisher, 2008a; 2008b), enhancing the quality of life of their wearers (Ahmad Najmee, Buari, Mujari, & Rahman, 2017) and being highly preferred for office work over single-vision spectacles (Kolbe & Degle, 2018; Sheedy & Hardy, 2005). Despite their extensive application, individuals adapt differently to the spatial distortions they generate (Alvarez, Kim, & Granger-Donetti, 2017), and some individuals may even experience swim balance issues, blurred vision, headaches, or waves of nausea (Han, Ciuffreda, Selenow, & Ali, 2003).

Some of these symptoms have been linked to the nonuniform optical magnification (Han et al., 2003), and the geometrical distortions that appear in the periphery of these lenses as they are produced (Esser, Becken, Altheimer, & Müller, 2017; Sheedy, Campbell, King-Smith, & Hayes, 2005; Sullivan and Fowler, 1988). Symmetry, orientation, and motion direction statistics of natural image sequences are all modified by the skew distortions in PALs and have been shown to produce skew

* Corresponding author at: Institute for Ophthalmic Research, Eberhard Karls University Tuebingen, Tuebingen 72076, Germany.
E-mail address: miguel.garcia-garcia@student.uni-tuebiengen.de (M. Garcia Garcia).

https://doi.org/10.1016/j.visres.2020.11.008
Received 4 May 2020; Received in revised form 28 October 2020; Accepted 7 November 2020
Available online 10 December 2020

aftereffects (Habtegiorgis et al., 2018; Habtegiorgis, Rifai, Lappe, & Wahl, 2018).

Geometric skew distortions like the ones in the periphery of the progressive addition lenses likely cause long term visual adaptation (Habtegiorgis et al., 2018). This might be important for the alteration in the peripheral motion perception (Habtegiorgis et al., 2018), some individuals experience while wearing these lenses. Because some PALs wearers report longer-lasting perceptual disturbances related to peripheral motion perception than others, it is crucial to better understand adaptation to complex motion stimuli in the peripheral visual field.

To perceive motion, information is integrated over space and time. This information can be spatiotemporal variations in luminance over time, or it can be a contrast or texture variation over time, (known as "first-order" and "second-order" motion respectively)(Hadad, Schwartz, Maurer, & Lewis, 2015). Motion perception has also been generally split into local and global perception, defined as the sensitivity to direction of motion in small regions, and the integration of disparate local motion signals, respectively (Adelson & Bergen, 1985; Anstis & Kim, 2011; Hedges et al., 2011). In addition to local and global motion, there is the interpretation of the change of an object's position over time ("object motion"). A more in-depth understanding of adaptation to distortions of moving natural scenes will need to consider how multiple types of motion interact and adapt together.

The curveball illusion (or double-drift illusion) involves both local and object motion and leads to a different perceptual interpretation when viewed foveally or in the periphery. The curveball illusion stimulus is comprised of an object changing position in one direction while its internal texture is moving in a different direction, much like a pitched baseball spinning while also moving through space. When viewed in the peripheral visual field, perception of the trajectory of the object is strongly, attractively influenced by the direction of the internal local motion. When viewed foveally, the local and object motion components can be dissociated, and the real trajectory of the object motion is perceived (Kozak & Castelo-Branco, 2009).

The curveball illusion was firstly described by De Valois (De Valois & De Valois, 1991) and subsequently revived by Shapiro et al. (Shapiro, Lu, Huang, Knight, & Ennis, 2010). Like the infinite regress illusion (Tse & Hsieh, 2006), an inability to resolve a conflict in the peripheral visual field leads to the illusory perception of a continuously receding object trajectory. Essentially, a "quirk" in the integration of two opposing types of information (S. M. Anstis, 1980) which can end up in a motion-induced perception shift (MIPS)(Chung, Patel, Bedell, & Yilmaz, 2007).

It is proposed that the perceived object motion is influenced by local motion inside the object under conditions of uncertainty about the precise position of the object (Cavanagh & Tse, 2019; Kwon, Tadin, & Knill, 2015). In this case, the strong local motion signal is combined with the object motion signal as the boundary between those components dilutes in the periphery (Shapiro, Knight, & Lu, 2011).

Why foveally segregated motion information is combined in the periphery is not yet fully understood. Despite this, there is evidence that the illusion is formed beyond early visual processing areas because the oculomotor system appears to be immune to the illusion because eye movements targeted at the stimulus are not influenced by the illusion (Lisi & Cavanagh, 2015). Nevertheless, the illusion's strength is not affected by visual attention (Haladjian, Lisi, & Cavanagh, 2018), suggesting that the illusion is constantly perceived in the periphery. Peripheral vision is usually known for having poor fine-detail acuity but higher contrast detection for moving textures (Finlay, 1982; Mckee & Nakayama, 1984), therefore it is appropriate that its duty was believed to be, particularly, to act as a specialised motion detector (Finlay, 1982). Understanding how geometric distortions change the combination of complex motions in the periphery may be an essential step in understanding how our visual system overcomes unpleasant distortions when introduced into the peripheral visual field. This study addresses the effect of geometrically skewed moving stimulus adaptation on the perception of the curveball illusion.

2. Material and methods

Seventeen participants (eight females and nine males, aged between 21 and 43 years, (mean = 28 years, SD = 5 years) took part in the study. In case they wore spectacle lenses (n = 2), the size of the stimuli was corrected, applying the magnification factor according to their foveal prescription.

None of the participants in the study reported any ocular complication or any medical condition that affected their normal vision or their motion judgements, such as cataracts, retinal or corneal dystrophies, epilepsy, or prior history of motion sickness.

2.1. Ethics

The study adhered to the tenets of the Helsinki Declaration (2013). The ethics authorisation to perform the measurements was granted by the Western Sydney University Human Research Ethics Committee with the ID H12292. Prior to data collection, the experiment was explained in detail to the participants, and written informed consent was collected from each participant. All data was pseudo-anonymised and stored in full compliance with the principles of the Data Protection Act GDPR 2016/679 of the European Union (The European Parliament and the Council of the European Union. (2016), 2016).

2.2. Apparatus

The experiment was developed in Matlab (R2019a) and Windows 10 (Build 17134) using the Psychophysics toolbox routines (Brainard, 1997; Kleiner, Brainard, Pelli, Ingling, & Murray, 2007) (Version 3.0.16) and the Eyelink toolbox (Cornelissen, Peters, & Palmer, 2002).

The experimental set-up consisted of a rear DLP LED ProPixx (VPixx Technologies, Saint-Bruno, Canada) projector mounted in a dark room, with a resolution of 1920 × 1080 pixels (Horizontal × Vertical), and a physical screen size of 1.325 × 0.735 m, whose diagonal pixel pitch was 0.6853 × 10–3 m, and running at a fixed nominal frame rate of 60 Hz. Observers sat at 1 m from the projector screen and placed their chins and forehead on a fixed chin-rest to maintain position stability.

Fixation was controlled by measuring gaze direction monocularly (left eye), with a long-range mounted Eye Link 1000 (SR Research, Ottawa, Canada) at a sampling rate of 500 Hz. All the settings are summarised in Appendix A.1.

2.3. Paradigm

Three different conditions were run in five independent sessions (conducted on different days, at approximately the same time of the day). The same set-up was used in all sessions. The order between sessions was randomised for each participant. Each session consisted of a pre-adaptation (baseline) measurement phase, an adaptation phase, and post-adaptation measurement phase with interleaved top-up stimuli. Fig. 1 displays the order of events within each session.

During the "baseline" phase of each session, the perceived verticality of a double-drift motion stimulus was determined by a two-alternative forced-choice (2AFC) decision after the presentation of the curveball illusion. The stimulus consisted of a vertically oriented Gabor presented within a circular Gaussian envelope moving downwards. At the same time, the inner texture of the Gabor drifted in an orthogonal direction (left or rightward motion). Participants were asked to respond via keyboard whether the ball/disc's final position was to the left or right of its original position after the descent. Then, a distortion adaptation session was introduced, where participants were exposed to distorted moving image content for a cumulative duration of 8 min (max. 13 min, depending on how good the subjects fixated on the centre of the screen). The third part of the experiment was identical to the first one, but with a top-up adaptation period of a minimum of 5 s of correct fixation between trials, in which distorted video content was shown. Proper fixation was

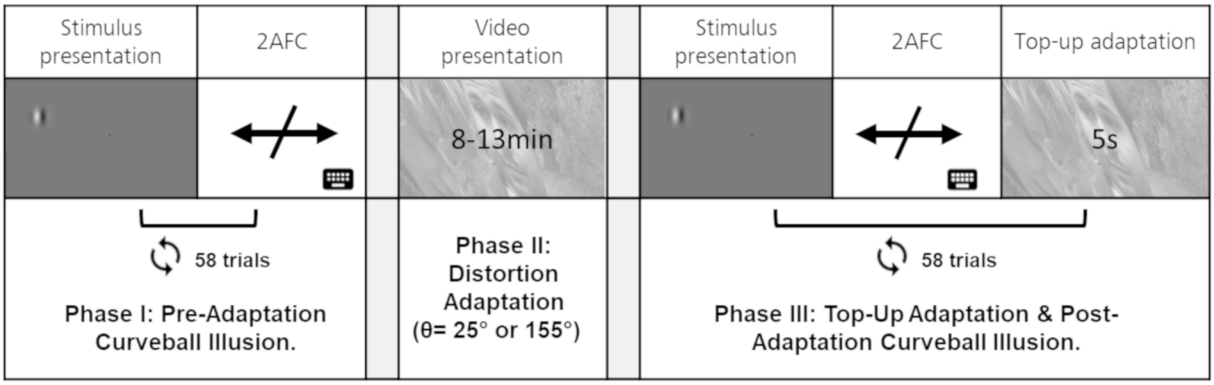

Fig. 1. Diagram showing the experimental session flow.

guaranteed at all time by gaze contingency, as trials were aborted if the participant stopped looking at the fixation target.

2.4. Stimuli

The double-drift stimulus was based on the original curveball illusion (Shapiro et al., 2010). It consisted of a Gabor patch of 3.5°diameter, containing two cycles per degree (cpd) at the maximum screen contrast. It was initially presented vertically positioned up 10°and horizontally displaced 20°from the central fixation point. Then, the Gabor translated down the screen at a fixed speed of 12,5 degrees per second until it reached a location 10°below centre. The centrally shown fixation target was a 10 pixels round black dot. The stimuli were presented on top of a homogeneous grey background. Unlike the original study (Shapiro et al., 2010), the vertical movement was not always straight but also included diagonal trajectories, allowing quantification of the object motion that was perceived as falling straight. The final horizontal position ranged from 5°to the left to 5°to the right, relative to the starting point. A total of 58 trials were assessed in each phase, and the distribution of the landing position was randomly determined over a Kaiser window with a shape factor $\beta = 3°$.

The adapting stimuli consisted of skewed natural image sequences from an open-source movie (Baumann, 2009). Each frame was distorted using an affine transformation as described by Habtegiorgis et al. (Habtegiorgis et al., 2017) and then cropped to the best-fitting size. The angle of the distortions applied was either + 25° (clockwise skew, Fig. 2c) or 155° (-25°, counterclockwise skew, Fig. 2b). In this study, no Hanning window was applied to the video, but rather it was presented at the full-screen size (Habtegiorgis et al., 2017; 2018). Hence, the field of view (FoV) covered by the video was around 66 by 40° (H × V). A schematic view of the video and the distortion components can be found in Fig. 2.

For the reader's convenience, all parameters from the video and the stimuli utilised in the different conditions are gathered in the appendix A.2.

2.5. Condition (1) – screen-left

Two sessions were collected under this condition, one for each movie distortion orientation. Aside from the common stimulus characteristics described above, during this condition, the stimulus was presented on the left side of the screen, and the inner structure of the Gabor had a

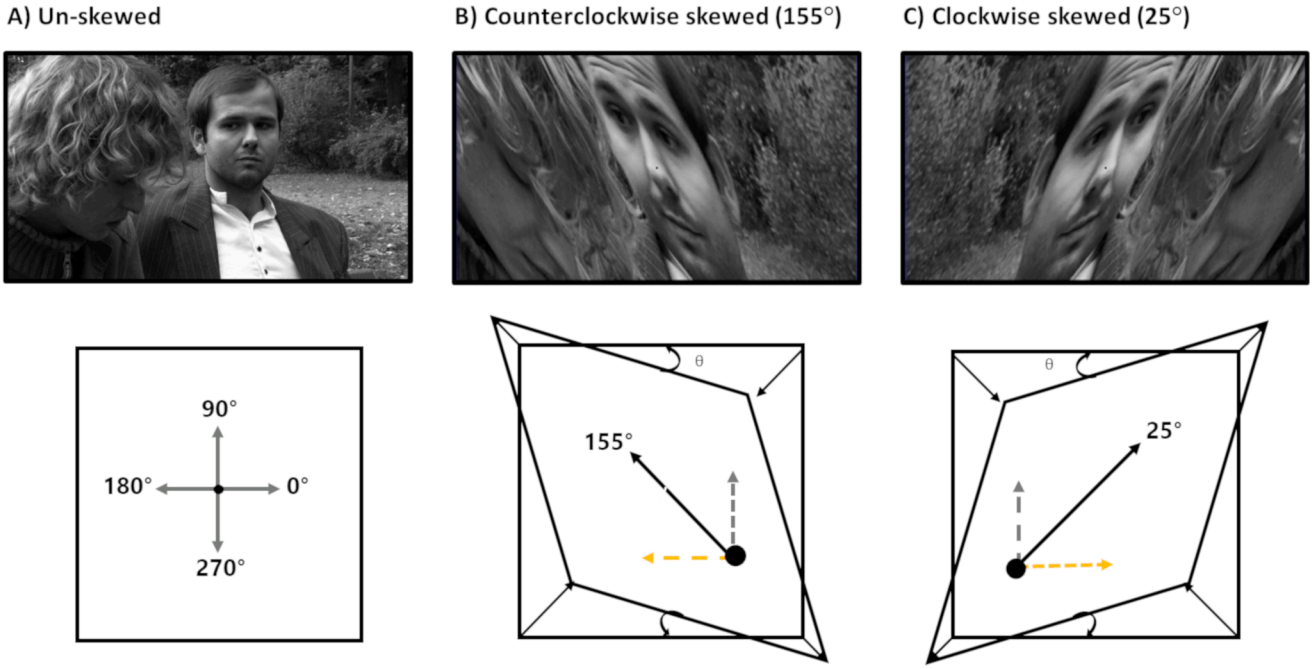

Fig. 2. Illustration of skew geometrical distortions, and examples frames. A) Original frame and reference frame B) Counterclockwise skew distortion ($\theta = 155°$ or $-25°$) and C) Clockwise skew distortion ($\theta = +25°$).

local motion component, where the texture of the Gabor drifted outbounding (from right to left) at a fixed speed of 20 degrees per second.

2.6. Condition (2) – screen-right

The paradigm followed was the same as in the screen-left condition, but the stimulus presentation was mirrored to the other side of the screen. Thusly, the double-drift stimulus of phases I and III of the experiment were presented on the right side of the screen, and the drift from the inner texture had its direction also changed to remain outbounding. Both movie distortion orientations were tested.

2.7. Condition (3) – no local motion (NLM)

Similar to the screen-left condition, but in this case, no local motion was present. Therefore, no drift was present in the inner structure of the Gabor patch. Instead, the stimulus was a static Gabor patch, moving vertically down. Only one adapting movie orientation was carried out with each participant, and this video orientation was randomly chosen (ABBA).

2.8. Analysis

For the analysis, the percentage of right versus left answers was calculated for each possible landing location of the stimulus. Then, a psychometric function (Wichmann & Jäkel, 2018) was fit using the Matlab package psignifit 4.0 (Schütt, Harmeling, Macke, & Wichmann, 2016). Default parameters were used to fit a cumulative Gaussian sigmoid with the maximum a posteriori estimators, following equation (1).

$$\Psi(x;m,w,\lambda,\gamma) = \gamma + (1-\lambda-\gamma)S(x;m,w); \quad S(x;m,w)=\Phi\left(c\frac{x-m}{w}\right); \quad c=\Phi^{-1}(95)-\Phi^{-1}(05) \tag{1}$$

Equation (1). Psychometric functions. Where ϒ is the lower bound, assumed to be zero in our case, and (1- λ) is the upper bound, a reflection of the lapse or error regardless of the stimulus intensity. Furthermore, x represents the stimulus level, m, and w, the threshold, and width, φ, and φ-1 are the cumulative standard normal distribution and its inverse.

The point of subjective equality (PSE (Ψ)) was defined at the 50% proportion of right vs left answers, indicating the object motion trajectory for which the participant perceived the ball as falling straight. From these PSEs, the overall effect of distortion adaptation on the double-drift illusion was estimated as the difference (Δ) between post- to pre-adaptation phases. One-sample Kolmogorov-Smirnov test was applied to ascertain the normality of the distributions of the PSEs and their differences.

Owing to the non-normal distribution of all the different conditions, non-parametric tests were used. In each session, the significance of aftereffects was determined by a Wilcoxon Signed-Rank test between the pre-adaptation PSE and the post-adaptation PSE. Differences between the point of subjective equality during the baseline conditions (screen left double-drift, screen right double-drift, and no local motion) were also tested with a Wilcoxon Signed-Rank test.

In order to establish the contribution of adaptation to changing the perceived direction of the local motion within the double-drift stimulus, the results from the 'Screen Right double-drift' condition were reversed and combined with the Screen Left condition. A paired signed-rank test was then performed to compare the PSE of the post-adaptation double-drift stimuli to the post-adaptation no local motion condition.

3. Results

3.1. Curveball illusion – Baseline conditions

Before adaptation, the baseline PSEs of the curveball illusion already varied between the screen-left (median PSE = 0.68) and screen-right condition (-0.94) (Signed-Rank; Z = 5.04, p < 0.01) (Fig. 3). When the local motion was translating leftward an object-motion with a rightward trajectory appeared to be travelling vertically down the screen. Meanwhile, a straight falling stimulus will be appreciated as biased to the left (clockwise trajectory). The opposite holds for the stimulus showing rightward translating local motion. The condition showing no local motion was only presented in the screen-left position, as such this is compared to the screen-left double-drift condition. As expected, without the local motion (-0.63) an object motion translating along a rightward tilted trajectory does not appear vertical. Indeed there appears to be a slight bias to perceive a left titled object trajectory as vertical, thereby producing a significant difference between the no local motion and screen-left double-drift baseline conditions. (Signed-Rank; Z = 4.43, p < 0.01). It is notable that the slope of the curve appears steeper in the no local motion condition, indicating that participants had better sensitivity in this condition relative to the double-drift condition.

3.2. Baseline consistency across sessions.

A simple linear regression across different sessions was calculated to estimate whether there was any reduction in the baseline illusion magnitude with exposure. Non-significant regression was found (F (1,67) = 0.111, p = 0.74) with an R2 of 0.0017. These results imply that the order of the sessions did not modify the strength of the curveball illusion measured during baseline conditions for the upcoming sessions, as there was no order reduction dependency.

3.3. Adapting condition (1) – screen-left (PRE-POST)

When the movie used during the adaptation phase had the horizontal component skewed in the opposite direction (25° or clockwise) to the local motion direction, the point of subjective equality was shifted by −0.89° (ΔPSE) from the baseline value (Z = 1.76, p = 0.08; Wilcoxon Signed-Rank). On the other hand, the video skewed 155° (or counter-clockwise), whose horizontal component was in the same direction, was

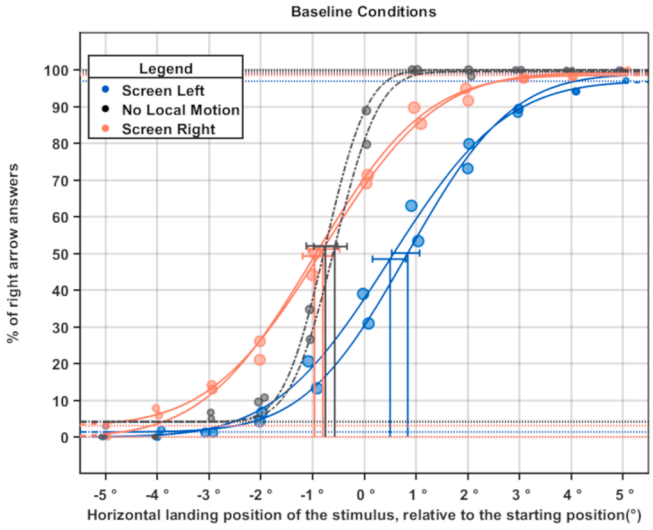

Fig. 3. Psychometric curves of the baseline conditions prior to adaptation. The 50% 'rightward' answers indicate the trajectory perceived as vertical. Participants completed these baseline measurements twice on separate days for each condition, represented by two curves for each condition to demonstrates the consistency of participants' responses for each condition. The No Local Motion condition was only measured once per participant; both curves indicate baseline measurements before one movie adaptor and the opposite one. The horizontal bars at the 50% values indicate the 95% CI for the fit of the pooling using all participants data. The size of the markers is proportional to the number of trials for the given stimuli parameters.

unable to modify the PSE from the baseline (ΔPSE = 0.01°; Z = -0.57, p = 0.57; Wilcoxon Signed-Rank). The psychometric curves are shown in Fig. 4. Here, in the case that the direction of skew is opposite to the direction of the local motion drift, we observe a repulsive aftereffect. In other words, after adaptation to a movie skewed in a clockwise direction, a stimulus that previously appeared to drift vertically down the screen now appears to drift to the right or along a counterclockwise tilted trajectory. Notably, this effect acted reducing the magnitude of the curveball illusion, while the counterclockwise adapter, on the other hand, did not induce a change in the strength of the curveball illusion.

3.4. Adapting condition (2) – screen-right (PRE-POST)

The screen-right condition differed from the screen-left condition in the location of the stimuli (right side of the screen) as well as the direction of the drift. Just as the test stimuli are physically mirroring the stimulus, the results also mirrored those obtained in the screen-left condition. Only the adapting movie whose horizontal component was oriented in the opposite direction of the drift (155° or counterclockwise) introduced a shift in the PSE (ΔPSE = 0.71°; Z = -2.291, p = 0.022; Signed-Rank) while the skew in the same direction (25°, clockwise) did not (ΔPSE = -0.01°; Z = 0.034; p = 0.973; Signed-Rank test). The psychometric curves are shown in Fig. 4.

3.5. Adapting condition (3) – no local motion (PRE-POST)

When the local motion component was not presented, both video adaptors introduced significant shifts in the perceived vertical object motion compared to the original perceived one. Before adaptation, a slight left-going object motion was perceived as vertical. After adaptation to the counterclockwise skewed movie (155°), post-test PSEs were significantly more positive (Δ = 0.73; Z = -2.38, p = 0.02; Signed-Rank test) indicating that a more straight-going object motion (i.e. a more counterclockwise tilted object translation) was now perceived as vertical. Meanwhile, the clockwise tilted (25°) movie produced a leftward shift in the PSE of Δ = -0.91, (Z = 2.04, p = 0.04; Signed-Rank test). The psychometric curves are shown in Fig. 4. This result demonstrates that despite some initial bias in the perceived vertical object motion when the test stimulus is on the left of the screen, both clockwise and counterclockwise skewed adaptors are capable of inducing an aftereffect of the perceived direction of object motion when no local motion is present to create the curveball illusion. Moreover, adaptation to a geometrically distorted movie stimulus produced a contrastive aftereffect whereby adaptation to a rightward (clockwise) skew caused a stimulus previously perceived as following a vertical trajectory to now appear to be following a counterclockwise trajectory.

3.6. Variation in the adaptation (No local motion vs local motion)

The no local motion condition shared the same location of the test stimuli as the screen-left condition. Hence, it allows for a direct comparison in the same hemifield and with the same adaptor, providing information about the contribution of the local motion component of the stimulus. Moreover, if the results from the right condition are inverted, it replicates those found in the screen-left condition, providing a more exhaustive analysis between local and no local motion effects. Non-significant differences were found between the strength of the aftereffects in combined local motion and no local motion conditions for any of the videos; 25° (p = 0.09; Signed-Rank) and 155°(p = 0.53; Signed-Rank).

4. Model

4.1. Contribution of local motion to the illusory perception

A model of the optic flow of the stimuli before adaptation was build to gain a better comprehension of how much local motion is modifying our perception of straightness during this optical illusion. For every condition, the theoretical optic flow was estimated by the summation of the horizontal and vertical motion vectors. The total components in every condition can be found in Table 1.

Then, using the results (PSEs) in the pre-adaptation periods for the Screen-Left and No Local Motion conditions and the equation (2), the contribution of the local motion component in the perception of the curveball illusion was estimated to be 1.7% ± 0.7% (mean; standard deviation).

$$\begin{bmatrix} \sum Vy_{PRE} \\ \sum Vy_{PRE} \end{bmatrix} = \begin{bmatrix} Vx_{LOCAL} \times \ Local\ Contribution \ + Vx_{GLOBAL} \\ \mathrm{Vy}_{LOCAL} \times \ Local\ Contribution \ + Vy_{GLOBAL} \end{bmatrix};$$

$$\theta_{PRE}(^{\circ}) = \ 360^{\circ} + atan\frac{\sum Vy_{PRE}}{\sum Vx_{PRE}} \times \frac{180}{\pi}; \tag{2}$$

$$PSE_{PRE} = \theta_{PRE}(^{\circ}) - 270^{\circ} + bias;$$

Table 1
Motion vector components of the physical double-drift stimuli.

Condition	Landing position (°)	Vx($^{\circ}s^{-1}$)Local motion	Vx2($^{\circ}s^{-1}$) Global motion	Vy($^{\circ}s^{-1}$) Global motion
NLM	0	0	0	−12.5
Left	0	−20	0	−12.5
Right	0	+20	0	−12.5

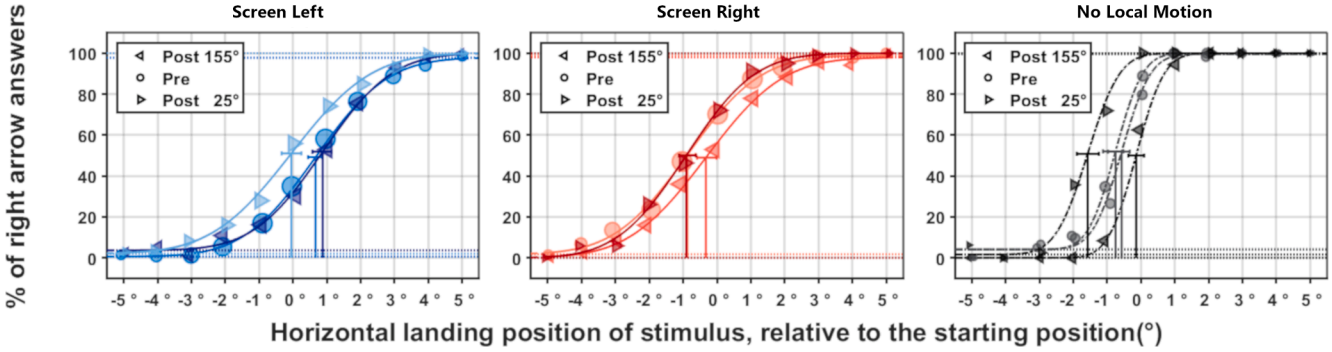

Fig. 4. Psychometric fits for the average response from all participants in the Screen-Left, Screen-Right and No Local Motion (NLM) conditions. X-label indicates the physical horizontal landing position of the stimulus where 0° indicates a vertical trajectory, positive values indicate a drift down to the right, and negative values indicate a drift down to the left. Y-label indicates the percentage of answers where participants pressed the right button. Marker sizes are proportional to the pooled number of responses. The right arrow indicates the clockwise adaptor skew orientation (25°) while the left arrow refers to the counterclockwise adaptor skew orientation (155°). Circles indicate the baseline condition.

Equation (2). Model to predict the shift in the stimulus perception due to the inclusion of a local motion component, where Vx and Vy indicate the motion components of the stimulus, the local contribution is the factor estimated, and the bias refers to the mean baseline PSE in the no local motion condition (~-0.79°).

4.2. Adaptation effects

The orientation of the vectors after exposure to the distorted movie can be estimated using Equation (3). Here, the same affine transformation that was used in the creation of the adaptation stimulus is applied to the moving components of the double-drift stimulus and then multiplied by a transfer factor. Finally, the difference between the angle of the stimulus post- adaptation and pre-adaptation is defined as the expected difference.

$$\begin{bmatrix} Vx_{POST} \\ Vy_{POST} \end{bmatrix} = \begin{bmatrix} Vx_{PRE} \\ Vy_{PRE} \end{bmatrix} \times \begin{bmatrix} 1 & -Mtan(\theta) \\ -Mtan(\theta) & 1 \end{bmatrix} \times \frac{1}{1-(Mtan(\theta))^2}; \tag{3}$$

$$\begin{bmatrix} \sum Vx_{POST} \\ \sum Vy_{POST} \end{bmatrix} = \begin{bmatrix} Vx^{POST}_{LOCAL} \times LocalContribution + Vx^{POST}_{GLOBAL} \\ Vy^{POST}_{LOCAL} \times LocalContribution + Vy^{POST}_{GLOBAL} \end{bmatrix};$$

$$\theta_{PRE}(^\circ) = 360^\circ + atan\frac{\sum Vy_{PRE}}{\sum Vx_{PRE}} \times \frac{180}{\pi};$$

$$\theta_{POST}(^\circ) = 360^\circ + atan\frac{\sum Vy_{POST}(\theta)}{\sum Vx_{POST}(\theta)} \times \frac{180}{\pi};$$

$$\Delta PSE(\theta) = \theta_{POST} - \theta_{PRE};$$

Equation (3). Model to predict the shift in stimulus perception after watching the skewed movie sequence, where Vx pre and Vy pre indicate the motion components of the stimulus, θ is the angle of the distortion and M is the adaptation transfer factor.

While the rest of the factors are given for this model, the adaptation transfer factor (M), or how much the visual system becomes tuned to the adaptor stimulus, is unknown. Adaptation to a geometrically distorted movie is likely to involve motion direction or motion streak adaptation predominantly but may also involve other forms of orientation and motion adaptation. For this reason, estimation of the adaptation transfer function was based on models of orientation and motion adaptation that describe a similar orientation dependence between different types of the adaptor and test stimuli (Clifford, Wenderoth, & Spehar, 2000). In this model, the adaptation transfer function was defined as a first derivative Gaussian function with a sigma factor = 40° (Tang, Dickinson, Visser, & Badcock, 2015). The relative difference in orientation between the adaptor and test stimulus being the essential factor in determining the strength of the adaptation, with maximum adaptation expected when the difference between the adaptor and test is 40°. When no local motion is present in the test stimulus, the relative difference in orientation between the distorted movie (adaptor) and the path of the test stimulus is 65° (as shown in Fig. 5i). In the screen-left condition, when the local motion is drifting to the left, the orientation of the test stimulus was estimated based on the perceived trajectory. The difference between the calculated orientation of the double-drift stimulus and the adaptor will be approximately 63°for the clockwise skewed and 67°the counter-clockwise orientation in the left condition, and vice versa for the Screen Right condition. The relationship between the stimulus-adaptor angle and the transfer factor can be observed in Fig. 5. The scaling factor of this Gaussian function was defined in a fashion that 65° matched the magnitude of adaptation observed in the median values of both orientations of no local motion condition. From there, the adaptation transfer factor values were estimated for the rest of the angles.

The model described above shows how the adaptation transfer factor would merely vary across the different movies and how it could vary if

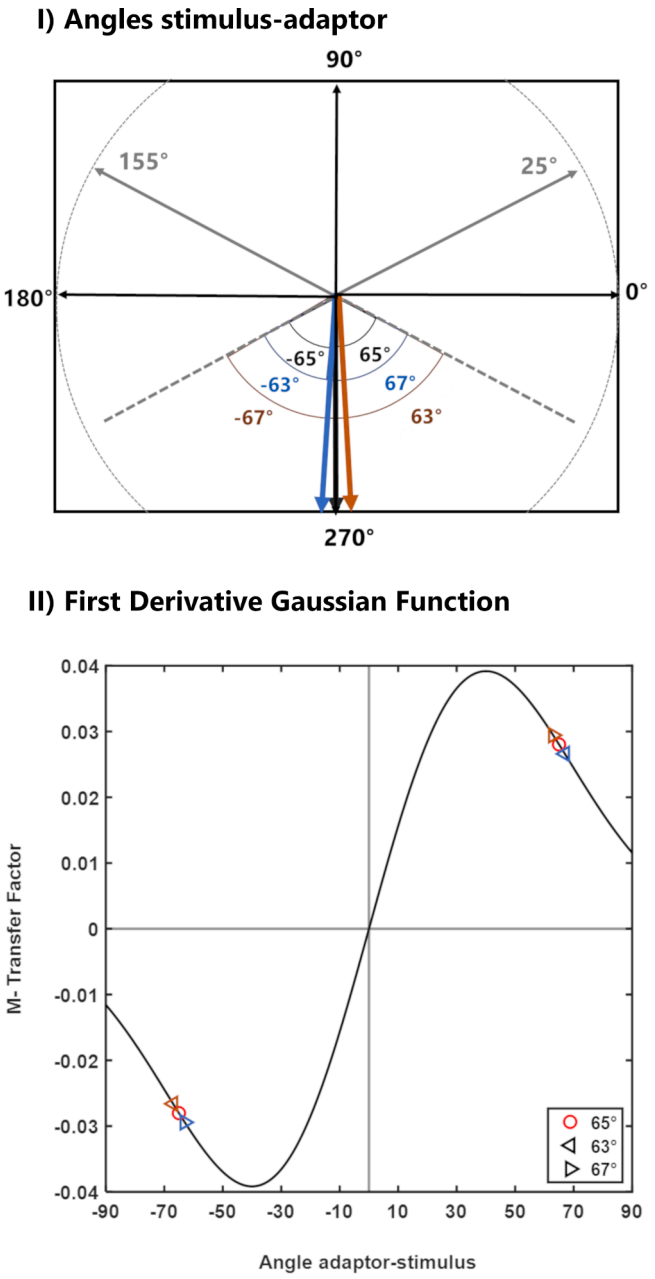

Fig. 5. I) The angle between perceived stimulus trajectory and video adaptor orientation for each condition measured, the blue line indicates the perceived trajectory from a straight falling double-drift illusion in the Screen Left baseline condition. In contrast, the orange line shows the perceived trajectory of the Screen Right baseline condition. II) Displays the first derivative Gaussian function that defines the adaptation transfer factor and its angular dependency.

different angles were chosen. Predicted strength of adaptation was accurately estimated in some but not all conditions. While predictions were off by<0.2° in the No Local Motion, Screen-Left & clockwise adapter and Screen-Right & counterclockwise adapter conditions, the model was not able to predict the results found when the movie adaptor presented a horizontal component skewed in the same direction as the local motion of the illusion, namely when the perception was not shifted. Table 2 presents the estimated values from the model, the measured ones, and their differences.

5. Discussion

This study aimed to explore how distortions, similar to those created

by daily-life optical solutions, can modify our perception of motion in complex situations. When the visual system is stimulated with a distorted input for a period of time, it becomes temporarily adapted. Consequently, our perception of stimuli temporarily shifts relative to perception prior to adaptation (Movshon & Lennie, 1979) in a self-calibration and decorrelation process (Barlow & Földiák, 1989) to maintain sensitivity in the face of a changing environment. These perceptual shifts of the visual system can be measured experimentally via aftereffects (Thompson & Burr, 2009). Prior studies have shown that adaptation to natural image sequences with geometrical skew distortions applied can elicit aftereffects in form and motion perception (Habtegiorgis et al., 2018). Here, the same geometrical skew distortions were able to produce a kind of direction aftereffect that affected the perception of the trajectory of an object translating down a projection screen. This aftereffect was repulsive in nature, where a previously vertically perceived movement is subsequently seen as translating along a trajectory that is opposite to the skew of the adapting movie. However, in the more complex cases, like when local motion is presented orthogonally to the global or object vertical motion (i.e.curveball or double-drift illusion), the adaptation occurs only when the orientation of the video distortion has a horizontal component "opposite" to the local motion direction, reducing the magnitude of the illusion. On the other hand, adaptation did not promote any change to the curveball illusion when the supplementary angle of distortion was applied, causing an asymmetry in the results.

To summarise these results, we find that a skewed, complex adapter can produce a direction aftereffect that tilts the perceived trajectory of an object moving down the screen. Nevertheless, when the test object comprises both local and object motion, adaptation appears to occur in an asymmetrical manner. In one case, adaptation follows the direction of the effect found when there was no local motion present in the test stimulus and acts to reduce the curveball illusion. In the other case, adaptation does not appear to impose any additional aftereffect, leaving the strength of the curveball illusion unchanged.

In the baseline conditions, namely, before adaptation to any distortion, a slight bias was found in the perception of the verticality of the stimulus. The nature of this bias seems to be dependent on the screen location as well as to the local motion component of the stimulus. When the local motion was not present, and the stimulus was positioned at the left side of the screen, the point of subjective equality was perceived at 0.63° (median NLM Baseline PSE) to the left (a leftward drift), rather than at zero degrees. A possible explanation for this metamorphopsia in the verticality judgement could be the orientation selectivity of the peripheral visual field (Simeonova & Vassilev, 1985; Yu & Rosa, 2014), or due to the aperture shape of the pupil contour (Oomes, Koenderink, van Doorn, & de Ridder, 2009; Wallach, 1935). Perception of "straightness" was then subsequently shifted when a local motion was present (curveball illusion) relative to this baseline distortion. When the stimulus texture drifted from right to left (as in the left condition), the PSE shifted from left of vertical to right of vertical(from −0.63° to 0.68°), producing an illusion of around 1.3°.

Additionally, by presenting an object motion stimulus similar to the curveball illusion stimulus but without the local motion component, we were able to calculate how much the local motion contributed to the illusion. Our data show a 1.7% (SD = ± 0.7%) contribution of the local motion into the final perception, which is relatively modest. Local and global motion are processed hierarchically within the visual system, with local signals being mostly handled in the primary visual cortex (V1) (Snowden, Treue, Erickson, & Andersen, 1991), while both, local and global, or combinatorial components are typically addressed by V5, also known as the motion area (Ajina, Kennard, Rees, & Bridge, 2015; Smith, Greenlee, Singh, Kraemer, & Hennig, 1998). In this case then, the contribution of area V1 to the judgements of MT+/V5, in terms of peripheral global motion perception, appears to be relatively small for our stimuli. Notably, the connections dedicated to peripheral vision in V1 going towards other cortical areas are relatively fewer in comparison with the central vision ones (Gurnsey & Biard, 2012; Shapiro et al., 2011).

Table 2
ΔPSE (°) for every condition, measured (mean values) and estimated from the model, and differences between both.

Condition	NLM 155	NLM 25	Left 25	Left 155	Right 25	Right 155
Measured	0.731	−0.914	−0.894	0.007	−0.099	0.708
Estimated	0.749	−0.749	−0.709	0.786	−0.786	0.709
Diff	0.018	0.165	0.185	0.779	0.687	0.001

Several authors have previously described an orientation dependency for tilt and motion aftereffects and modelled them using a first-derivative of a Gaussian (Clifford et al., 2000; Tang et al., 2015). It is not clear exactly which perceptual 'features' might be adapted by our complex skewed adapter, but it seems reasonable to expect that motion direction tuned mechanisms are adapted. This orientation dependency was included in our model, but it could not account for the asymmetry that our results presented. Owing to the nature of our stimuli, the angle between adaptor and stimulus would be almost symmetric in every condition. Therefore, the aftereffects with both adapting movies should have been similar in magnitude. As outlined above, this was found not to be the case. However, there are other possible explanations for why one of the adapting orientations did not have any effect over the double-drift illusion.

When we observed adaptation to the skewed movie, the result was a decreased curveball illusion, but the illusion did not entirely vanish. The remnant of the illusion can be observed by the fact that the post adaptation PSEs of the Screen-Left condition were still different from those found in the baseline of the NLM (No local motion) condition. Furthermore, the magnitude of the shift that occurs in these Screen-Left and the Screen-Right conditions (+25° in the Screen Left and + 155° in the Screen Right condition) are similar in magnitude to the shift produced by the adaptation of object motion alone. These shifts might suggest that only the object motion is adapted to the skew and that local motion is not adapted. If this were the case, in the opposite adaptation condition (+155° in the Screen Left and + 25° in the Screen Right condition) a much larger illusion would be expected after adaptation.

In the 'no local motion' conditions, we find that the object motion trajectory adapts symmetrically. Using the double-drift test stimulus, there is a lack of a strengthened illusion in the counterclockwise adapter (Screen Left) and clockwise adapter (Screen Right) conditions. Assuming that the object motion trajectory does adapt symmetrically, we would need to consider that either the local motion contribution to the illusion is affected by the skew of the adapter or that the double-drift stimulus is affecting the adaptation process.

On the one hand, the post-adaptation outcome could be a cumulative effect from adaptation and the test stimulus. Hence, what appears to be a lack of change in the size of the illusion would rather be a change in the driver of the illusion. If the skew of the movie introduces a biased horizontal motion component that matches the direction of the local motion in the test stimulus, the sensitivity to this motion in the test stimulus would be reduced. But when the skew of the movie introduces a biased horizontal motion component that is opposite (180°) to the direction of the local motion in the test stimulus, the sensitivity could be retained.

Alternatively, the adaptation process could have interacted asymmetrically with the local properties of the test stimulus by modifying the spatial coding along the perceived trajectory of the test. Kosovicheva et al. (Kosovicheva, Maus, Anstis, Cavanagh, Tse, & Whitney, 2012) found that tilt aftereffects can be induced in the illusory location of an adapter shifted by a motion-induced position perception shift. The tilt-aftereffect (TAE) induced in the perceived location of the adapting stimulus was greater than in the 'antiperceived' location. If the global properties of the adapter were to induce adaptation even to local visual features along with the adapted skew orientation, this would also

produce an asymmetrical aftereffect. I.e. when the motion trajectory perceived as vertical after adaptation matches (or is close to matching) the motion trajectory perceived as vertical during the curveball illusion, along that trajectory, the local stimulus properties may be adapted in a complex way so as to be unable to contribute further to the illusion. On the other hand, when the motion trajectory perceived as vertical after adaptation does not match the motion trajectory perceived as vertical during the curveball illusion, the local stimulus properties may remain capable of contributing to the illusion. In the circumstances created in this experiment, thereby balancing with the object motion trajectory aftereffect to apparently reduce the strength of the illusion.

Another suggestion for the asymmetry could be that it is not possible to induce a stronger illusion than the one our stimulus already elicits in the baseline conditions because the illusorily vertical stimulus would require an oblique trajectory that travels toward the fovea, where uncertainty would be less. However, we consider this explanation to be unlikely because the stimulus was at minimum 15°in the periphery and Shapiro et al. (Shapiro et al., 2010) found a consistently symmetrical illusion, no matter whether the inner texture drifted towards or away from the fovea.

The study presents some potential limitations that should be acknowledged as they could have influenced our results. For instance, greater population samples could have lead to normal distributions, slightly more clear shifts and the possibility to analyse inter-individual differences. Due to the same problem, significance was not reached at a 95% significance level between the Pre-Post adaptation in the Screen Left condition and the distortion orientation of 25°. We take this shift to be true, however, given the proximity in the p-value (0.07) and the clear shift in the median values.

Finally, the curveball illusion was known to increase in effect with eccentricity for a fixed stimulus size (Shapiro et al., 2010) but to decrease as the stimulus size grows (Gurnsey & Biard, 2012). Likewise, as the local motion speed is reduced, the magnitude of the illusion slightly decreased (Shapiro et al., 2010). In future, while measuring the curveball illusion, adaptation to a prior stimulus should be taken into account, or even participants who wear progressive addition lenses should be analysed in a different group.

6. Conclusions

In conclusion, the geometrical skew distortions used in this study have proven themselves capable of modifying not only object motion perception but also the perception of illusory motion, under certain conditions. The double-drift illusion was reduced after being adapted to geometrical distortions to a specific orientation but not strengthened with the opposite orientation. This orientation dependency implies that not only the angle of overall distortion but also the type and angle of individual stimulus components play a role in the visual tuning of this asymmetrical curveball aftereffect. Finally, it should be taken into account that the distortions presented here can also be found in the progressive addition lenses. The adaptation to these lenses in a real-world environment is likely to involve a complex combination of components in the visual scene leading to asymmetrical and complex perceptual effects, possibly contributing to habituation problems in the progressive lens wear.

Author contributions

MGG, KR, TW, and SW, conceived the experiment. MGG & TW conducted the experiment. KR, TW & SW participate in the funding acquisition, project administration and supervision. Every author participated in the elaboration of the manuscript and reviewed the submitted version.

CRediT authorship contribution statement

Miguel Garcia Garcia: Conceptualization, Data curation, Software, Formal analysis, Visualization, Investigation, Methodology, Validation, Writing - original draft, Writing - review & editing. **Katharina Rifai:** Conceptualization, Supervision, Methodology, Project administration, Funding acquisition, Writing - original draft. **Siegfried Wahl:** Supervision, Project administration, Funding acquisition, Writing - review & editing. **Tamara Watson:** Conceptualization, Resources, Methodology, Validation, Supervision, Funding acquisition, Project administration, Writing - original draft, Writing - review & editing.

Declaration of Competing Interest

The authors declare that there are no conflicts of interest that could have interfered in the course of this study.

Acknowledgements

This work was supported by the European Grant PLATYPUS (Grant Agreement No 734227), a Marie Sklodowska-Curie RISE initiative. Authors M.G.G., K.R. & S.W. are employed by Carl Zeiss Vision International GmbH (E) and are scientists at the University Tuebingen. T.W. is employed (E) by Western Sydney University. According to the journal policy, they declare their employment positions.

The authors acknowledge support by Open Access Publishing Fund of the University of Tubingen.

The founders did not have any additional role in the study design, data collection, and analysis, decision to publish, or preparation of the manuscript. The specific roles of these authors are articulated in the 'author contributions' statement.

Appendix A. 0.1

Parameters	Values
Screen	
Type of projection	Rear
Resolution	1920 × 1080 pixels
Physical size of the screen	1.325 × 0735 *m*
Distance to the screen	1 *m*
Estimated D/W	1.3947
DPI	36
Dot pitch (H, V, D)	0.6901×10^{-3} *m*0.6806 × 10^{-3} *m*0.6853 × 10^{-3} *m*
Frame rate (nominal)	60 Hz
Real monitor refresh interval (a.k.a IFI)	0.0083sec/frame
Maximum brightness	600 lm
Contrast*	2000:1
Bit depth	16

(*continued on next page*)

(*continued*)

Parameters	Values
Eye Tracker Settings	
Eye tracked	OS
Lens mounted	–
Distance to the eye	1 *m*
Frequency of refresh	500 Hz
Calibration	5 points

Appendix A. 0.2

Parameters	Values
CurveBall stimuli	
Texture grating spatial frequency	2 cpd
Michelson Contrast	100%***
Diameter	3.5°
Initial position horizontal	20° Leftwards*
Initial position vertical	10° Superior *
Final position vertical	10° Inferior*
Range of landing destinations horizontal	[-5°: 1: +5°]**
Distribution of the stimuli	Kaiser ($\beta = 3°$)
* In reference to the fixation point. ** In reference to the starting position. *** In reference to max and minimum from the projector.	
Motion/ Double-drift	
Local motion (Horizontal spin/drift)	$20°s^{-1}$
Global motion (Vertical speed)	$12.5°s^{-1}$
Video Stimuli	
Aspect ratio	16:9
FoV Covered	66° x 40°
Source	Valkaama
Distortions applied (angle)	$\Theta = [155° \| \| 25°]$

Refraction errors for the two subjects wearing spectacles were: SEQ = -3 dpt & −4 dpt respectively for both eyes of each participant.

References

Adams, W. J., Banks, M. S., & van Ee, R. (2001). Adaptation to three-dimensional distortions in human vision. *Nat Neurosci, 4*(11), 1063–1064. https://doi.org/10.1038/nn729.

Adelson, E. H., & Bergen, J. R. (1985). Spatiotemporal energy models for the perception of motion. *Journal of the Optical Society of America A: Optics, Image Science, and Vision, 2*(2), 284. https://doi.org/10.1364/JOSAA.2.000284.

Ahmad Najmee, N. A., Buari, N. H., Mujari, R., & Rahman, M. I. (2017). Satisfaction Level of Progressive Additional Lens (PALs) Wearers. Environment-Behaviour Proceedings Journal, 2(6), 373. https://doi.org/10.21834/e-bpj.v2i6.999.

Ajina, S., Kennard, C., Rees, G., & Bridge, H. (2015). Motion area V5/MT+ response to global motion in the absence of V1 resembles early visual cortex. Brain, 138(1), 164–178. https://doi.org/10.1093/brain/awu328.

Alvarez, T. L., Kim, E. H., & Granger-Donetti, B. (2017). Adaptation to Progressive Additive Lenses: Potential Factors to Consider. *Scientific Reports, 7*(1), 1–14. https://doi.org/10.1038/s41598-017-02851-5.

Anstis, S. M. (1980). The perception of apparent movement. *Philosophical Transactions of the Royal Society of London. Series B, Biological Sciences, 290*(1038), 153–168. https://doi.org/10.1098/rstb.1980.0088.

Anstis, S., & Kim, J. (2011). Local versus global perception of ambiguous motion displays. Journal of Vision, 11(3), 13. https://doi.org/10.1167/11.3.13.

Barlow, H. B., & Földiák, P. (1989). Adaptation and decorrelation in the cortex. In R. Durbin, C. Miall, & G. Mitchison (Ed.), The Computing Neuron (pp. 54-72). Wokingham, England: Addison-Wesley. The Computing Neuron, 54–72.

Baumann, T. (2009). Chancen von Open Source Software Geschäftsmodellen und Entwicklungsansätzen in der Filmindustrie. http://www.valkaama.com/files/paper/Tim_Baumann_-_Open_Source_Film_-_Diplomarbeit_16.02.2009.pdf.

Brainard, D. H. (1997). The Psychophysics Toolbox. *Spatial Vision, 10*(4), 433–436. http://www.ncbi.nlm.nih.gov/pubmed/9176952.

Cavanagh, P., & Tse, P. U. (2019). The vector combination underlying the double-drift illusion is based on motion in world coordinates: Evidence from smooth pursuit. *Journal of Vision, 19*(14), 2. https://doi.org/10.1167/19.14.2.

Chung, S. T. L., Patel, S. S., Bedell, H. E., & Yilmaz, O. (2007). Spatial and temporal properties of the illusory motion-induced position shift for drifting stimuli. *Vision Research, 47*(2), 231–243. https://doi.org/10.1016/j.visres.2006.10.008.

Clifford, C. W. G., Wenderoth, P., & Spehar, B. (2000). A functional angle on some after-effects in cortical vision. *Proceedings of the Royal Society of London, Series B: Biological Sciences, 267*(1454), 1705–1710. https://doi.org/10.1098/rspb.2000.1198.

Cornelissen, F. W., Peters, E. M., & Palmer, J. (2002). The Eyelink Toolbox: Eye tracking with MATLAB and the Psychophysics Toolbox. *Behavior Research Methods, Instruments, & Computers : A Journal of the Psychonomic Society Inc, 34*(4), 613–617. http://www.ncbi.nlm.nih.gov/pubmed/12564564.

De Valois, R. L., & De Valois, K. K. (1991). Vernier acuity with stationary moving Gabors. *Vision Research, 31*(9), 1619–1626. https://doi.org/10.1016/0042-6989(91)90138-U.

Esser, G., Becken, W., Altheimer, H., & Müller, W. (2017). Generalization of the Minkwitz theorem to nonumbilical lines of symmetrical surfaces. *Journal of the Optical Society of America. A, Optics, Image Science, and Vision, 34*(3), 441–448. https://doi.org/10.1364/JOSAA.34.000441.

Finlay, D. (1982). Motion Perception in the Peripheral Visual Field. *Perception, 11*(4), 457–462. https://doi.org/10.1068/p110457.

Gurnsey, R., & Biard, M. (2012). Eccentricity dependence of the curveball illusion. *Canadian Journal of Experimental Psychology, 66*(2 SPL.ISSUE), 144–152. https://doi.org/10.1037/a0026989.

Habtegiorgis, S., Erlenwein, C., Rifai, K., & Wahl, S. (2018). Interaction between form and motion processing contributes to habituation to distortions of the natural visual world. *Journal of Vision, 18*(10), 626. https://doi.org/10.1167/18.10.626.

Habtegiorgis, S. W., Rifai, K., Lappe, M., & Wahl, S. (2017). Adaptation to Skew Distortions of Natural Scenes and Retinal Specificity of Its Aftereffects. *Frontiers in Psychology, 8*, 1158. https://doi.org/10.3389/fpsyg.2017.01158.

Habtegiorgis, S. W., Rifai, K., Lappe, M., & Wahl, S. (2018). Experience-dependent long-term facilitation of skew adaptation. *Journal of Vision, 18*(9), 7. https://doi.org/10.1167/18.9.7.

Hadad, B., Schwartz, S., Maurer, D., & Lewis, T. L. (2015). Motion perception: A review of developmental changes and the role of early visual experience. In Frontiers in Integrative Neuroscience (Vol. 9, Issue SEP, pp. 1–18). Frontiers Research Foundation. https://doi.org/10.3389/fnint.2015.00049.

Haladjian, H. H., Lisi, M., & Cavanagh, P. (2018). Motion and position shifts induced by the double-drift stimulus are unaffected by attentional load. *Atten Percept Psychophys, 80*(4), 884–893. https://doi.org/10.3758/s13414-018-1492-0.

Han, Y., Ciuffreda, K. J., Selenow, A., & Ali, S. R. (2003). Dynamic interactions of eye and head movements when reading with single-vision and progressive lenses in a simulated computer-based environment. *Investigative Ophthalmology and Visual Science, 44*(4), 1534–1545. https://doi.org/10.1167/iovs.02-0507.

Hedges, J., Gartshteyn, Y., Kohn, A., Rust, N., Shadlen, M., Newsome, W., & Movshon, J. A. (2011). Dissociation of Neuronal and Psychophysical Responses to Local and Global Motion. *Current Biology, 21*(23), 2023–2028. https://doi.org/10.1016/j.cub.2011.10.049.

Kleiner, M., Brainard, D., Pelli, D., Ingling, A., Murray, R., & C, B. (2007). What's new in psychtoolbox-3. Perception, 36(14), 1–16.
Kolbe, Oliver, & Degle, Stephan (2018). Presbyopic Personal Computer Work: A Comparison of Progressive Addition Lenses for General Purpose and Personal Computer Work. *Optometry and Vision Science, 95*(11), 1046–1053. https://doi.org/10.1097/OPX.0000000000001295.
Kosovicheva, A. A., Maus, G. W., Anstis, S., Cavanagh, P., Tse, P. U., & Whitney, D. (2012). The motion-induced shift in the perceived location of a grating also shifts its aftereffect. Journal of Vision, 12(8), 7–7. https://doi.org/10.1167/12.8.7.
Kozak, Lajos R., & Castelo-Branco, Miguel (2009). Peripheral Influences on Motion Integration in Foveal Vision Are Modulated by Central Local Ambiguity and Center-Surround Congruence. *Investigative Ophthalmology & Visual Science, 50*(2), 980. https://doi.org/10.1167/iovs.08-2094.
Kwon, Oh-Sang, Tadin, Duje, & Knill, David C. (2015). Unifying account of visual motion and position perception. *Proceedings of the National academy of Sciences of the United States of America, 112*(26), 8142–8147. https://doi.org/10.1073/pnas.1500361112.
Lisi, Matteo, & Cavanagh, Patrick (2015). Dissociation between the Perceptual and Saccadic Localization of Moving Objects. *Current Biology, 25*(19), 2535–2540. https://doi.org/10.1016/j.cub.2015.08.021.
Mckee, Suzanne P., & Nakayama, Ken (1984). The detection of motion in the peripheral visual field. *Vision Research, 24*(1), 25–32. https://doi.org/10.1016/0042-6989(84)90140-8.
Meister, Darryl J, & Fisher, Scott W (2008a). Progress in the spectacle correction of presbyopia. Part 1: Design and development of progressive lenses. *Clinical and Experimental Optometry, 91*(3), 240–250. https://doi.org/10.1111/j.1444-0938.2007.00245.x.
Meister, Darryl J, & Fisher, Scott W (2008b). Progress in the spectacle correction of presbyopia. Part 2: Modern progressive lens technologies. *Clinical and Experimental Optometry, 91*(3), 251–264. https://doi.org/10.1111/j.1444-0938.2008.00246.x.
Movshon, J. Anthony, & Lennie, Peter (1979). Pattern-selective adaptation in visual cortical neurones. *Nature, 278*(5707), 850–852. https://doi.org/10.1038/278850a0.
Ohlendorf, Arne, Tabernero, Juan, & Schaeffel, Frank (2011). Neuronal adaptation to simulated and optically-induced astigmatic defocus. *Vision Research, 51*(6), 529–534. https://doi.org/10.1016/j.visres.2011.01.010.
Oomes, Augustinus H J, Koenderink, Jan J, van Doorn, Andrea J, & de Ridder, Huib (2009). What are the Uncurved Lines in Our Visual Field? A Fresh Look at Helmholtz's Checkerboard. *Perception, 38*(9), 1284–1294. https://doi.org/10.1068/p6288.
Poullain, A. G., & Cornet, D. H. J. (1911). Optical lens. (Patent No. US1143316A). https://patents.google.com/patent/US1143316A/en?oq=U.S.+Patent+No.+1%2c143%2c316.
Schütt, Heiko H., Harmeling, Stefan, Macke, Jakob H., & Wichmann, Felix A. (2016). Painfree and accurate Bayesian estimation of psychometric functions for (potentially) overdispersed data. *Vision Research, 122*, 105–123. https://doi.org/10.1016/j.visres.2016.02.002.
Shapiro, A., Lu, Z.-L. L., Huang, C.-B. B., Knight, E., & Ennis, R. (2010). Transitions between central and peripheral vision create spatial/temporal distortions: A hypothesis concerning the perceived break of the curveball. PLoS ONE, 5(10), e13296. https://doi.org/10.1371/journal.pone.0013296.
Shapiro, A. G., Knight, E. J., & Lu, Z. L. (2011). A first- and second-order motion energy analysis of peripheral motion illusions leads to further evidence of "feature blur" in peripheral vision. PLoS ONE, 6(4), e18719. https://doi.org/10.1371/journal.pone.0018719.
Sheedy, James E., Campbell, Charles, King-Smith, Ewen, & Hayes, John R. (2005). Progressive Powered Lenses: The Minkwitz Theorem: *Optometry and Vision Science, 82*(10), 916–922. https://doi.org/10.1097/01.opx.0000181266.60785.c9.
Sheedy, James E., & Hardy, Raymond F. (2005). The optics of occupational progressive lenses. *Optometry - Journal of the American Optometric Association, 76*(8), 432–441. https://doi.org/10.1016/j.optm.2005.06.012.
Simeonova, B., & Vassilev, A. (1985). Perception of line orientation in the center and periphery of the visual field. *Acta Physiologica et Pharmacologica Bulgarica, 11*(2), 3–10. http://www.ncbi.nlm.nih.gov/pubmed/4050467.
Smith, Andrew T., Greenlee, Mark W., Singh, Krish D., Kraemer, Falk M., & Hennig, Jürgen (1998). The Processing of First- and Second-Order Motion in Human Visual Cortex Assessed by Functional Magnetic Resonance Imaging (fMRI). *Journal of Neuroscience, 18*(10), 3816–3830. https://doi.org/10.1523/JNEUROSCI.18-10-03816.1998.
Snowden, R. J., Treue, S., Erickson, R. G., & Andersen, R. A. (1991). The response of area MT and V1 neurons to transparent motion. *Journal of Neuroscience, 11*(9), 2768–2785. https://doi.org/10.1523/JNEUROSCI.11-09-02768.1991.
Sullivan, C. M., & Fowler, C. W. (1988). Progressive addition and variable focus lenses: 8 (1916), 402–414.
Tang, M. F., Dickinson, J. E., Visser, T. A. W., & Badcock, D. R. (2015). The broad orientation dependence of the motion streak aftereffect reveals interactions between form and motion neurons. Journal of Vision, 15(13), 1–18. https://doi.org/10.1167/15.13.4.
The European Parliament and the Council of the European Union. (2016). Regulation (EU) 2016/679 of the European Parliament and of the Council. Official Journal of the European Union, 59(L119/1).
Thompson, P., & Burr, D. (2009). Visual aftereffects. In Current Biology (Vol. 19, Issue 1, pp. R11–R14). Cell Press. https://doi.org/10.1016/j.cub.2008.10.014.
Tse, P. U., & Hsieh, P.-J. (2006). The infinite regress illusion reveals faulty integration of local and global motion signals. *Vision Research, 46*(22), 3881–3885. http://www.ncbi.nlm.nih.gov/pubmed/16879854.
Wallach, H. (1935). Über visuell wahrgenommene Bewegungsrichtung. *Psychologische Forschung, 20*(1), 325–380. https://doi.org/10.1007/BF02409790.
Webster, M. A., Georgeson, M. A., & Webster, S. M. (2002). Neural adjustments to image blur. *Nature Neuroscience, 5*(9), 839–840. https://doi.org/10.1038/nn906.
Wichmann, F. A., & Jäkel, F. (2018). Methods in Psychophysics. In Stevens' Handbook of Experimental Psychology and Cognitive Neuroscience. https://doi.org/10.1002/9781119170174.epcn507.
Yu, H. H., & Rosa, M. G. P. (2014). Uniformity and diversity of response properties of neurons in the primary visual cortex: Selectivity for orientation, direction of motion, and stimulus size from center to far periphery. *Visual Neuroscience, 31*(1), 85–98. https://doi.org/10.1017/S0952523813000448.